6th March 2026
Department of Physics, Faculty of Science, University of Split

PHOTOCLIM 3rd Annual meeting

PRESENTATION OF THE RESULTS ACHIEVED DURING THE SECOND PROJECT YEAR

Project funded by the Croatian Science Foundation IP-2022-10-8859

Fragility of primary production under climate change

PHOTOCLIM

PHOTOCLIM.ORG

HrZZ

Croatian Science Foundation

Visit project website for news: photoclim.org

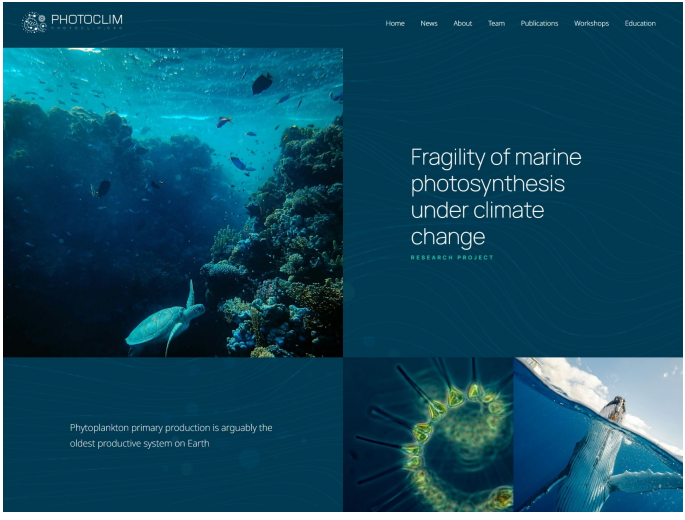

Second year work plan

List of deliverables:

D13. Annual project work meeting
D14. Filling data gaps in the local database
D15. Creating time series of photosynthesis parameters
D16. Creating time series of Gaussian parameters
D17. Workshop on bioeconomic models in oceanography
D18. Creating a theoretical framework for quantifying the discount rate of marine ecosystems
D19. Workshop on primary production modeling
D20. Educational materials on dynamic models of primary production
D21. Training in primary production measurements at the Plymouth Marine Laboratory
D22. Training in primary production modelling at the Plymouth Marine Laboratory
D23. Attendance at conferences
D24. Scientific publication
D25. Scientific publication

D13. Annual project work meeting

On the **20th February 2025** we had our Annual meeting at the Faculty of Science in Split.

Meeting agenda

09:30 – 10:00 Gathering of participants
10:00 – 10:05 Opening remarks
10:05 – 10:30 Presentation of the results achieved in the first project year
Presentation of the work plan for the remaining project period
Presentation of the financial plan for the remaining project period
11:00 – 11:30 Coffee & Discussion
11:30 – 12:30 Planning of Project Activities for the Second Year
Filling in data gaps
Creating time series of photosynthesis parameters
Creating time series of Gaussian parameters
Software tools for data processing
12:30 – 13:00 Planning of the workshop project - Modeling of primary production
13:00 – 15:00 Lunch

D14. Filling data gaps in the local database

Stončica	1962	
Kaštelanski zaljev	1962	
Bermuda Atlantic Time Series	1988	bats.bios.edu
Hawaii Ocean Time Series	1988	hahana.soest.hawaii.edu/hot/hot-dogs
Cariaco	1996	imars.marine.usf.edu/car
Monterey Bay	1988	www.mbari.org/bog
La Coruña	1990	www.seriestemporales-ieo.com
Western Channel Observatory	1992	www.westernchannelobservatory.org.uk

D15. Creating time series of photosynthesis parameters

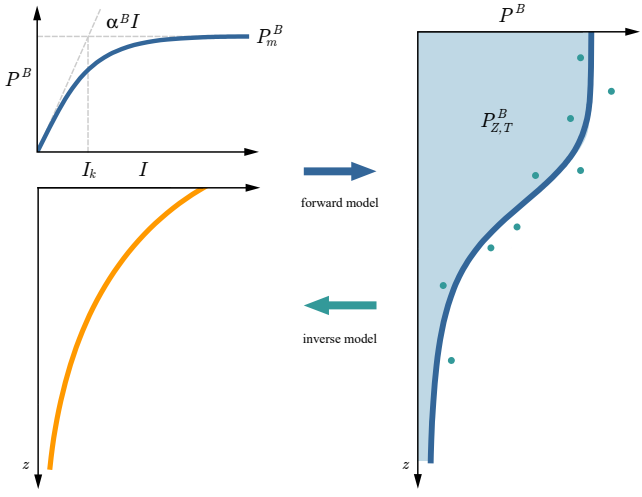

D15. Creating time series of photosynthesis parameters

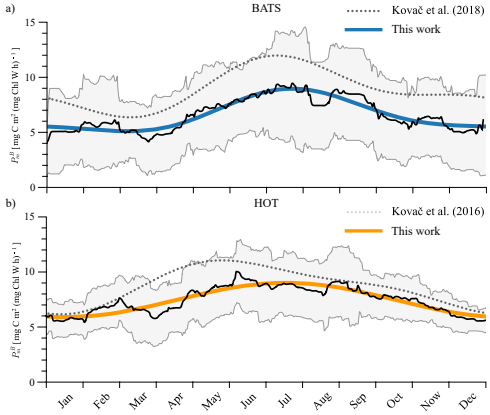

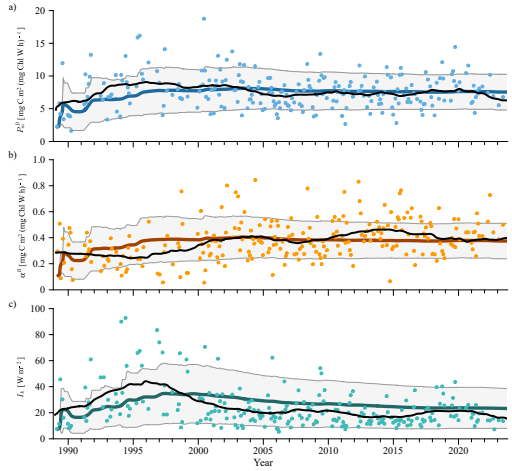

D15. Creating time series of Gaussian parameters

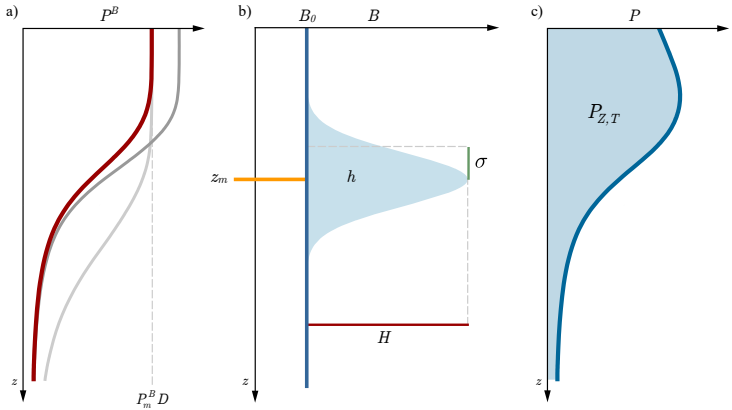

D17. Workshop on bioeconomic models in oceanography

On the 5th September at the Faculty of Science we have held the **Bioeconomical models in oceanography workshop**. The workshop hosted experts from physics, biology and economics, which together discussed the topic of sustainable usage of marine resources in a changing world.

A detalied report from the workshop can be found here:
www.photoclim.org/news/workshop-on-bioeconomical-models-in-oceanography

D17. Workshop on bioeconomic models in oceanography

Bioeconomic interpretation of primary production models

Žarko Kovač[1], Davor Mance[2], Diana Mance[3,*], Shubha Sathyendranath[4], Anja Kovač [5]

[1] *Faculty of Science, University of Split, Rudera Boškovića 33, 21000 Split, Croatia*
[2] *University of Rijeka, Faculty of Economics, Ivana Filipovića 4, 51000 Rijeka, Croatia*
[3] *University of Rijeka, Faculty of Physics, Department of Environmental Sciences, Radmile Matejčić 2, 51000 Rijeka, Croatia*
[4] *Plymouth Marine Laboratory, Prospect Place, The Hoe, Plymouth PL1 3DH, UK*
[5] *Institute of Oceanography and Fisheries, Šetalište Ivana Meštrovića 63, 21000 Split, Croatia*
[*] **corresponding author: diana.mance@uniri.hr**

Under review in Ecological Modelling

D19. Modelling primary production workshop

From the 27th to 31st October we have held the **Modelling primary production workshop**. The theme of the workshop was primary production modelling with a strong emphasis on parameter estimation methods for fine tuning of primary production models.

A detalied report from the workshop can be found here:
https://www.photoclim.org/workshops/modelling-primary-production/

D19. Modelling primary production workshop

D20. Educational material on primary production modelling

Our second educational material is now available for download!

Modelling Primary Production

https://www.photoclim.org/education/

D20. Educational materials on dynamic models of primary production

Following (3.16) and integrating the previous expression (over time and depth) yields the mixed layer production:

$$P_{Z_m,T} = \int_0^{Z_m}\int_0^{D} P(z,t)\,\mathrm{d}t\,\mathrm{d}z = \frac{Ba^B I_T}{K}(1 - e^{-KZ_m}), \tag{5.2}$$

where I_T stands for the total available light energy at the surface received during one day:

$$I_T = \int_0^{D} I_0(t)\,\mathrm{d}t. \tag{5.3}$$

Now assume, in line with Figure 21, a depth-independent, biomass-specific, **loss rate** L^B, such that the total loss $L(z,t)$ at each depth and time is given by:

$$L(z,t) = BL^B, \tag{5.4}$$

where L^B is the loss rate per unit biomass in the broadest sense (respiration, grazing), which can be parametrized in numerous ways [62]. Integrating this expression (over time and depth) yields mixed layer losses as:

$$L_{Z_m,T} = \int_0^{Z_m}\int_0^{D} L(z,t)\,\mathrm{d}t\,\mathrm{d}z = BL^B_T Z_m, \tag{5.5}$$

with $L^B_T = 24\,L^B$, where the 24 comes due to integration over the entire day. We stress that temporal integration is carried out over daylight hours for primary production and over 24 hours for the loss term.

Following Sverdrup [58] the **critical depth** Z_c (m) is defined as the depth for which the following holds:

$$P_{Z_c,T} = L_{Z_c,T}, \tag{5.6}$$

or stated explicitly for Sverdup's model:

$$\frac{a^B I_T}{K}(1 - e^{-KZ_c}) = 24\,L^B Z_c. \tag{5.7}$$

The obtained equation is a transcendental one. Luckily, it is solvable using the Lambert W function, but prior to presenting the exact solution we will first interpret this expression.

For active mixing proceeding exactly to the critical depth $Z_m = Z_c$, mixed layer production equals losses and therefore no biomass accumulation takes place. In order for biomass accumulation to take place, production needs to exceed losses:

$$\frac{a^B I_T}{K}(1 - e^{-KZ_m}) > 24\,L^B Z_m, \tag{5.8}$$

which occurs when mixing does not proceed to the critical depth $Z_m < Z_c$. If mixing proceeds beyond the critical depth $Z_m > Z_c$ losses dominate:

$$\frac{a^B I_T}{K}(1 - e^{-KZ_m}) < 24\,L^B Z_m, \tag{5.9}$$

and biomass accumulation will not take place. To know which condition is satisfied we proceed to solve (5.7) to obtain Z_c.

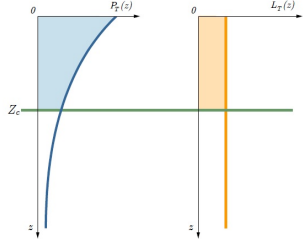

Figure 22: Graphical representation of the critical depth Z_c (green line) as the depth at which vertically integrated production (blue surface) equals vertically integrated losses (orange surface).

D20. Educational materials on dynamic models of primary production

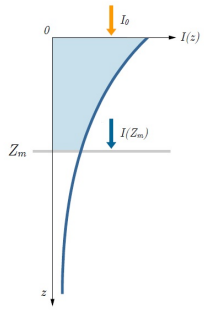

Figure 28: Irradiance at the mixed layer depth $I(Z_m)$ (blue arrow) calculated using expression (6.8), based on surface irradiance (orange arrow) attenuated due to water and mixed layer biomass.

Combining the previous two expressions we derive the following expression for average biomass at steady state:

$$B^* = \frac{K_W}{k_B}\left(\frac{C}{Z_m} - 1\right). \tag{6.14}$$

It is important to note that this result is general and does not depend on the specific formulation of the photosynthesis irradiance function. The production light relation, as dictated by the photosynthesis irradiance

function determines C and therefore B^*. We stress that C is the optically uncoupled critical depth and is the solution to:

$$\int_0^C P^B(I)\,\mathrm{d}z = L^B C, \tag{6.15}$$

under irradiance attenuated only due to water:

$$\frac{\mathrm{d}I}{\mathrm{d}z} = -K_W I, \tag{6.16}$$

implying that biooptical coupling is not present in the model. With no biooptical coupling irradiance at C is simply:

$$I(C) = I_0 \exp\left(-K_W C\right). \tag{6.17}$$

By expressing $I^*(Z_m)$ from (6.13) at steady state, we arrive at:

$$I^*(Z_m) = I_0 \exp\left(-K_W C\right). \tag{6.18}$$

We observe that irradiance at the mixed layer depth at steady state equals the irradiance at the optically uncoupled critical depth:

$$I^*(Z_m) = I(C). \tag{6.19}$$

This result was already demonstrated for the linear photosynthesis irradiance model (5.32). Here we see it is generalized to any photosynthesis irradiance function.

Finally, having derived the solution for average steady state biomass, it is straightforward to find the total steady state biomass, by simply multiplying (6.14) with the mixed layer depth (Figure 29):

$$B^*_Z = \frac{K_W}{k_B}\left(C - Z_m\right). \tag{6.20}$$

According to this expression total steady state biomass is proportional to the depth difference between the optically uncoupled critical depth and the mixed layer depth. In case of a mixed layer approaching zero the solution gives:

$$\lim_{Z_m \to 0} B^*_Z = \frac{K_W}{k_B} C. \tag{6.21}$$

This is a finite quantity, in comparison to the solution for average steady state biomass (6.14), which diverges when Z_m goes to zero.

D20. Educational materials on dynamic models of primary production

7.3 THE EFFECT OF SINKING ON THE BIOMASS PROFILE

Let us assume the phytoplankton sink with a **sinking speed** w ($\mathrm{m\,s^{-1}}$). For now, assume that biomass is conserved, such that neither production nor losses affect B. In this case we can write:

$$B(z, t + \Delta t) = B(z - w\Delta t, t) \tag{7.17}$$

This expression states that biomass at depth z and time $t + \Delta t$ came from depth $z - w\Delta t$ and time t (Figure 39). In the limit of small Δt, Taylor series expansion of both sides around $B(z, t)$ gives:

$$B(z, t) + \frac{\partial B}{\partial t}\Delta t \approx B(z, t) - w\frac{\partial B}{\partial z}\Delta t. \tag{7.18}$$

Cancelling terms on both sides yields the **advection equation**:

$$\frac{\partial B}{\partial t} + w\frac{\partial B}{\partial z} = 0. \tag{7.19}$$

The exact solution to this equation, under no flux boundary condition at the surface, is set by the initial condition $B_0(z)$ and reads:

$$B(z, t) = B_0(z - wt). \tag{7.20}$$

It is important to stress that the shape of the initial condition does not change with time, it simply gets advected with depth. Therefore, the ultimate fate of any phytoplankton is to sink out of the photic zone (Figure 39).

Now assume that during Δt production and losses also affect B. Equation (7.17) now becomes:

$$B(z, t + \Delta t) = B(z - w\Delta t, t)\left[1 + \frac{1}{\chi}\left(P^B(z - w\Delta t, t) - L^B\right)\Delta t\right]. \tag{7.21}$$

This expression states that during sinking, production acts to increase biomass and losses act to decrease biomass. Phytoplankton that started off at depth $z - w\Delta t$ and time t will experience production given by $B(z - w\Delta t, t)P^B(z - w\Delta t, t)$ and losses given by $B(z - w\Delta t, t)L^B$. Once

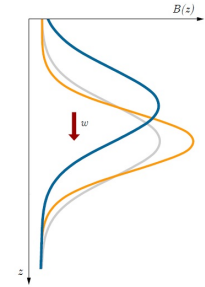

Figure 39: Subjected to sinking the phytoplankton will simply be "washed out" out of the photic zone. Each phytoplankton cell increases its depth due to sinking w (red arrow). The biomass profile (blue curve) gets advected with depth (grey curve), but it also changes shape due to production and losses during sinking (orange curve).

again, in the limit of small Δt, Taylor series expansion of both $B(z, t)$ and $P^B(z, t)$ gives:

$$\begin{aligned} B(z, t) + \frac{\partial B}{\partial t}\Delta t \approx\ & B(z, t) - w\frac{\partial B}{\partial z}\Delta t \\ & + \frac{1}{\chi}\left[B(z, t) - w\frac{\partial B}{\partial z}\Delta t\right]\left[P^B(z, t) - w\frac{\partial P^B}{\partial z}\Delta t\right]\Delta t \\ & + \frac{1}{\chi}\left[B(z, t) - w\frac{\partial B}{\partial z}\Delta t\right]L^B\Delta t. \end{aligned} \tag{7.22}$$

Marija Bačeković Koloper attended the following training programs:

12th to 16th May 2025.
Training in primary production measurements at the Plymouth Marine Laboratory

8th to 16th September 2025.
Training in primary production modelling at the Plymouth Marine Laboratory

D23. Attendance at conferences: IOCS 2025

Robert Brewin gave a keynote lecture titled Aquatic Carbon from Space. Shubha Sathyendranath was part of the Planning Comittee. Žarko Kovač presented a poster titled: Towards analysis ready primary production data, while Marija Bačeković Koloper presented a poster titled: Bayesian Estimation of Photosynthesis–Irradiance Parameters for Marine Phytoplankton.

D24. Scientific paper on time series of photosynthesis parameters

Time series of photosynthesis parameters

Žarko Kovač[1], Anja Kovač[2], Marin Vojković[1,*], Leon Ćatipović[1], Marija Bačeković Koloper[1], Shubha Sathyendranath[3,4]

[1] *Faculty of Science, University of Split, Rudera Boškovića 33, 21000 Split, Croatia*
[2] *Institute of Oceanography and Fisheries, Šetalište I. Meštrovića 63, 21000 Split, Croatia*
[3] *Plymouth Marine Laboratory, Prospect Place, The Hoe, Plymouth PL1 3DH, UK*
[4] *National Centre for Earth Observations, Plymouth Marine Laboratory, Prospect Place, The Hoe, Plymouth PL1 3DH, UK*
[*] **corresponding author: mvojkovic@pmfst.hr**

Under review in Journal of Geophysical Research: Oceans

D24. Scientific paper on time series of photosynthesis parameters

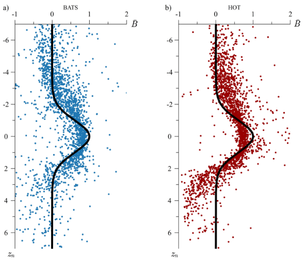

Figure 4: Comparison of modelled (black curve) versus measured chlorophyll at depth for: a) BATS (blue points) and b) HOT (red points). The black curve corresponds to the Gaussian function with zero mean and unit standard deviation. In order to show the chlorophyll measurements on the same plot, all data were normalized as described in detail in the text. The coefficient of determination for BATS is 85.32 % and for HOT it is 88.49 %.

model is adequate to describe the measurements and subsequently the optimal parameter values are well suited for modelling primary production at these two stations, with the proviso that the parameters be paired with the same model that was used to retrieve them (Kovač et al., 2017b). In this instance, the model used here falls in the class of non-spectral models for light penetration and photosynthesis, with the exponential function (11) used to describe the photosynthesis irradiance curve (Platt et al., 1980).

To highlight the overall fit of daily production with depth (12) we proceeded to normalize primary production data in a similar fashion as was done for the chlorophyll data, as shown in Figure 4. The procedure for normalization of production data is given in great detail in Kovač et al. (2016b). In short, the result of normalization allows for a direct comparison of the f_z function (13) with measured daily production at each individual depth. The results are provided in the Supplementary material (Supplementary figures 3 and 4). As can be seen from the Supplementary figures the normalized data follows well the production at depth as predicted by (13) and the model displays no bias.

We have also checked the model data mismatch over time to see if there is evidence of a temporal bias. We found no temporal bias, implying that the parameters are suitable for a time-series analysis, which is treated in the next section.

3.2 Seasonal cycle

The seasonal cycle of parameters at both stations are examined first, followed by an analysis of the entire time series. As already mentioned, due to the lack of sufficient PAR data we were not able to estimate reliably the seasonal cycle of the initial slope and the photoadaptation parameter at BATS. But it was possible for the HOT time series, and the photoadaptation parameter was derived from the initial slope and the assimilation number.

The irregular sampling intervals, with the average monthly frequency (Figure 1.a) and gaps in the data (Figures 1.b and 1.c), make the estimation of the mean, median and variance for each month difficult. For a given month, calculations imply taking all the values that were measured in that given month over all the years. However, for an ocean station which is sampled at irregular intervals and has gaps, such as the two stations here, this procedure may result in erro-

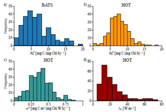

Figure 5: Histograms of the recovered photosynthesis parameters at BATS and HOT. a) Histogram of the assimilation number at BATS. b) Histogram of the assimilation number at HOT. c) Histogram of the initial slope at HOT. d) Histogram of the photoadaptation parameter at HOT. The initial slope and the photoadaptation parameter were not estimated at BATS due to a lack of optical data needed to accurately estimate their values.

neous estimation of the seasonal cycle. The reason is that, if there is significant variability at time scales shorter than one month, the sampling at irregular intervals may yield results that may be more noisy than the original data. Also, as evident by the tails in the distributions of parameters (Figures 4 and 5) there is higher probability than normal for low or high parameter values. Due to these reasons, we may get erroneous estimates of the mean, median or variance for a given month using the this approach.

To tackle these problems we estimated the mean seasonal cycle of parameter values by calculating the mean value for each day of the year, taking into account data collected 15 days prior and 15 days post a given day, over all years, following the approach of Kovač et al. (2016b) and Kovač et al. (2018b). In this manner, the effect on the estimation of the mean on that day, caused by scarce data is minimised. The results are shown in Figure 7. At BATS the assimilation number P_m^B has a minimum in March and maximum in July. At HOT the minimum in P_m^B is in January and the maximum is in June. The initial slope α^B did not have a strong seasonal cycle at HOT, while at BATS we were unable to estimate it due to the lack of optical data. Seasonal cycles of watercolumn production at both stations, estimated in the same manner, are given in the Supplementary material (Supplementary figures 1 and 2).

In comparison to the previous results of Kovač et al. (2018b), obtained on a ten-years-shorter time series at BATS, the seasonal cycle of the assimilation number is rather similar in phase, albeit different in magnitude (Figure 7.a). For BATS the difference in the magnitude is pronounced throughout the year and during the maximum in July the difference is most pronounced. For HOT the difference from Kovač et al. (2016b) results occur both in phase and in amplitude (Figure 7.b). The prior observed maximum was in May and now we observe it in July. Apart from the phase shift in the maximum, a significant difference in the amplitude is not observed over the entire year.

The photoadaptation parameter I_k did not have a clearly defined seasonal cycle at HOT, as was observed earlier by Kovač et al. (2016b). However, the minimum in January

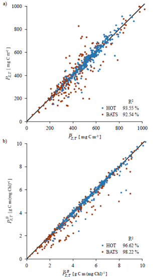

Figure 6: Model versus data comparison for: a) watercolumn production $P_{Z,T}$ and b) normalized watercolumn production $P_{Z,T}^B$ at both stations. Tilde marks the measured variable, whereas the model variable is without a tilde. Data from BATS are given in red and data from HOT are given in blue. The coefficient of determination R^2 for each station is given in the bottom right corner.

and a maximum in June were also observed in this work (not shown). It is important to stress that the photoadaptation parameter is the ratio of the assimilation number to the initial slope (14), with the initial slope being a rather small number in comparison with the assimilation number. Therefore, a small error in the estimated value of the initial slope may lead to a large error in the estimated value of photoadaptation parameter. Since the estimation of the assimilation number by the inverse method is more robust than the estimation of the initial slope (Kovač et al., 2017b), the error in the estimation of the initial slope has a stronger effect on the photoadaptation parameter.

Along the lines of Kovač et al. (2016b) and Kovač et al. (2018b), we fitted a sum of two sine functions to the seasonal cycles of the assimilation number: first with an annual period and the second with a semi annual period (Figure 7). For HOT only one sine function was sufficient to model the seasonal cycle, namely the one with the annual period, while

Under review in Journal of Geophysical Research: Oceans

D25. Scientific paper on the determination of photosynthesis parameters from a global database

A new global dataset of photosynthesis parameters

Žarko Kovač[1], Marija Bačeković Koloper[1,*], Shubha Sathyendranath[2,3], Gemma Kulk[2,3], Heather Bouman[4], Leon Ćatipović[1]

[1]*Faculty of Science, University of Split, Rudera Boškovića 33, 21000 Split, Croatia*
[2]*Plymouth Marine Laboratory, Prospect Place, The Hoe, Plymouth PL1 3DH, UK*
[3]*National Centre for Earth Observations, Plymouth Marine Laboratory, Prospect Place, The Hoe, Plymouth PL1 3DH, UK*
[4]*Department of Earth Sciences, University of Oxford, Oxford, OX1 3AN, UK*
[*]**corresponding author: mbacekovi@pmfst.hr**

Under review in Earth System Science Data

D25. Scientific paper on the determination of photosynthesis parameters from a global database

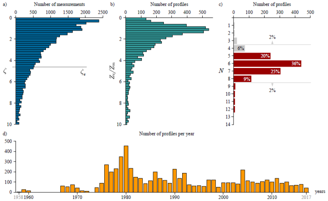

Figure 4: Plots of auxiliary variables. a) Histogram of measurement depths expressed as optical depths. Each individual measurement is treated as one entry. Euphotic zone ζ_e is highlighted by the grey line. b) Histogram of the ratio between the euphotic depth and the mixed layer depth. Here each profile is treated as one entry. c) Histogram of profiles with a given number of measurement depths. The two grey arrows indicate that percentages refer to all the profiles below or above the grey line. d) Time series of the number of measured production profiles per year globally.

values of photosynthesis parameters, the measured production profile has to have a minimal number of depths to vertically resolve the shape of the normalised production profile. As demonstrated by Kovač et al. (2016b) the normalised production profile (6) is uniquely determined by the photosynthesis parameters, whereas normalised daily watercolumn production (8) is not. This is because the normalised watercolumn production is an integral of the normalised production profile (Figure 1) and therefore loses the degrees of freedom that are present in the production profile, which enable the estimation of photosynthesis parameters. Therefore, a given pair of photosynthesis parameters may not be an exact match for the normalised production profile, but it may be a good match for watercolumn production.

We have analysed the distribution of profiles with respect to the number of measurement depths per profile, as shown in Figure 4.c. The highest number of profiles has 6 measurement depths, which is adequate for successful parameter estimation. The total number of profiles with 6 or more measurement depths accounts for 72% of the measured profiles. Around 20% of the profiles have 5 measurement depths, which is on the limit for successful parameter estimation. In order to use as much of the available data as possible, we have opted to use these profiles as well in parameter estimation. The remainder 8% of profiles have less than 5 measurement depths. In other words, out of the 6 084 profiles, 473. For these profiles, it is not feasible to estimate both parameters, and therefore we opted to exclude them. On the other end, some profiles have measurements from 9 to 14 depths (which is excellent), but these account for less than 2% of all the profiles.

Looking at the temporal distribution of measurements, as shown in Figure 4.d, the observations start in 1958, but there is a gap from 1961 till 1966, with another gap year in 1973. After 1975, there is a surge in data collection, with the highest number of profiles being measured in 1980 and in the neighbouring years. Afterwards, the global number of measured profiles is of the order of 100 per year. This is arguably very low, highlighting the value of such measurements, given the high demand for photosynthesis parameters in remote sensing applications and in ecosystem models. With this in mind, we now proceed to describe the application of the inverse model and the obtained results.

4 Results

As a first step in the application of the inverse model we have analysed primary production profiles for signs of vertical homogeneity in photosynthesis parameters, by testing whether they meet condition (12), and if so for how many depths. Out of the total 5611 profiles with more than 4 measurement depths, 988 profiles do not violate this condition at all, 2407 profiles violate it at one depth, 1469 at two depths and 747 at three or more depths. We have at first applied the inverse model on all profiles only to find that those profiles which strongly violate the vertical homogeneity condition result in outlier values for photosynthesis parameters. Therefore, we focus on those profiles for which

the vertical homogeneity condition is not violated, or violated at one or two depths. In total there are 4864 such profiles. This accounts for 80% of the original 6084 profiles in the Mattei & Scardi (2021) dataset.

Distributions of photosynthesis parameters obtained from these profiles are provided in Figure 5. The obtained parameter values are within the expected ranges thus far reported in the literature (Kovač et al., 2017b; Bouman et al., 2018; Amirian et al., 2025). The estimated values of the initial slope α^B range from above 0 to 0.6 $\mathrm{mg\,C\,(mg\,Chl)^{-1}\,(W\,m^{-2})^{-1}\,h^{-1}}$, with only a handful parameter values above the upper limit. The majority of values of the assimilation number P_m^B are found to be below 10 $\mathrm{mg\,C\,(mg\,Chl)^{-1}\,h^{-1}}$, with the bulk of the estimates being above 0 and below 5 $\mathrm{mg\,C\,(mg\,Chl)^{-1}\,h^{-1}}$, consistent with conventional photosynthesis-irradiance experiments. Neither of these parameters are normally distributed, being positively skewed and exhibiting long tails. The mean and median of the inital slope α^B being 0.194 and 0.130 $\mathrm{mg\,C\,(mg\,Chl)^{-1}\,(W\,m^{-2})^{-1}\,h^{-1}}$, respectively, with the mean and median of the assimilation number P_m^B begin 4.315 and 2.736 $\mathrm{mg\,C\,(mg\,Chl)^{-1}\,h^{-1}}$, respectively. From the information on the values of the initial slope and the assimilation number it is straightforward to calculate the photoadaptation parameter, defined as:

$$I_k = \frac{P_m^B}{\alpha^B}. \tag{17}$$

The photoadaptation parameter describes how phytoplankton adjust their light-harvesting capacity to ambient light conditions (Reynolds, 2006; Kirk, 2011). It represents the irradiance at which phytoplankton transition from light limited to light saturated photosynthesis (Jassby & Platt, 1976) and is also a measure of the light level to which phytoplankton have adapted (Zonneveld, 1997). Distribution of the photoadaptation parameter is also given in Figure 5. It is positively skewed with a long tail. The bulk of the photoadaptation parameter values are found below 50 $\mathrm{W\,m^{-2}}$. The mean and the median are 20.862 and 11.615 $\mathrm{W\,m^{-2}}$, respectively.

We stress here that the objective of this study was not to provide an interpretation of this specific dataset, but rather to increase the number of photosynthesis parameters available for usage in primary production models. A comprehensive interpretation of the estimated parameter values would necessitate a detailed oceanographic analysis and knowledge of regional, or local biogeochemical processes, which falls outside the scope of the present work and is a potential course for future research. To facilitate this, we provide the obtained parameter values in a table published online at https://zenodo.org/records/17973417 (Kovač et al., 2025). Along with each estimated pair of photosynthesis parameters we provide the original profile number given by Mattei & Scardi (2021) so that the parameter values can be traced back to the profiles from which they had been estimated. We also give the date of each profile, along with coordinates. To be more precise the data are comprised of the following: date (year, month, day), latitude, longitude, initial slope α^B, assimilation number P_m^B and the original profile number from Mattei & Scardi (2021), each given in a separate column. We only provide parameter values in which both parameters were estimated successfully, in line with the limitations set by the experiment and the inverse procedure, described in detail in (Kovač et al., 2016b). We

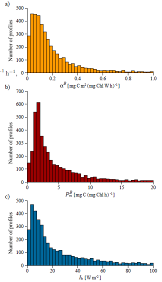

Figure 5: Histograms of the estimated photosynthesis parameters: a) Distribution of the initial slope α^B, b) Distribution of the assimilation number P_m^B, c) Photoadaptation parameter I_k. The horizontal axis shows parameter values, and the vertical axis indicates the percentage of profiles within each interval of those values.

also flag the values where the inverse procedure did not result in realistic values of photosynthesis parameters with 0, the ones where the initial slope is too high with 0.5 and the realistic values with 1.

In the provided table, parameter values for which the inverse model did not converge onto realistic values are flagged and given as NaN. In some of these cases the model did yield reasonable estimates for watercolumn production, but for unrealistic values of photosynthesis parameters. This occurs due to the fact that watercolumn production is not uniquely determined by the photosynthesis parameters, but the production profile is (Kovač et al., 2016b). Therefore, the method may converge on a combination of parameter values for which watercolumn production is estimated rather well, but the production profile is not. In short, for those cases, the model gives the correct answer for watercolumn production, but for the wrong reasons. Keeping in mind the parameter values are estimated from the shape of the production profile we consider the error in the profile to

D26. Additional result: Project application accepted

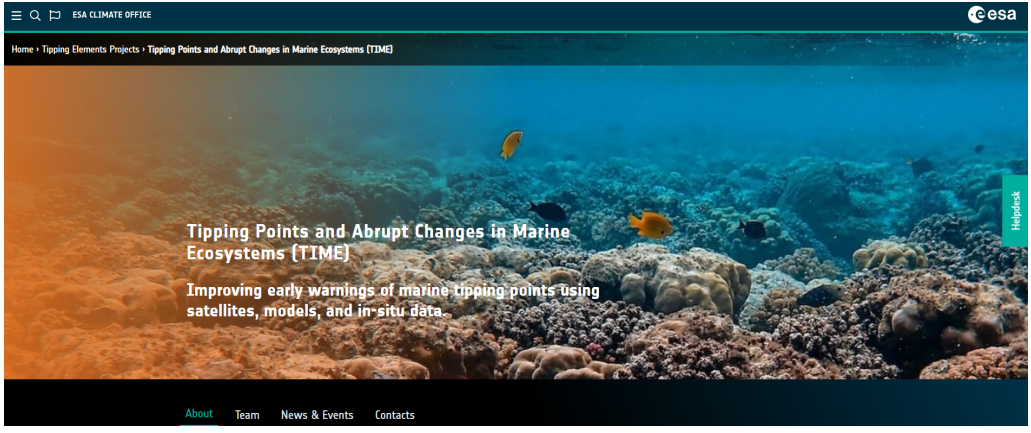

D27. Additional result: New project application

A new project application to the COST call Open Call Collection OC-2025-1 called the **Pan-European Research Alliance for Antifragile Systems Methods (MANTIS)** was submitted. Associates from 13 countries participated in the project application. The project team includes Žarko Kovač, whose role is the application of stochastic models in the study of antifragility of primary production in the sea. The project provides financial resources for networking with foreign partners on topics close to the PHOTOCLIM project.

Island Trapped Waves Enhance Primary Production in Idealized Numerical Models

Jasen R. Jacobsen[1,*], Christopher A. Edwards[1], Žarko Kovač [2], Hrvoje Mihanović[3], Zrinka Ljubešić[4]

[1]University of California, Santa Cruz, 1156 High St, Santa Cruz, CA 95064, USA

[2]University of Split, Ul. Boškovića 31, 21000, Split, Croatia

[3]Institute of Oceanography and Fisheries, šetalište Ivana Meštrovića 63, 21000, Split, Croatia

[4]University of Zagreb, Faculty of Science, Horvatovac 102A, Zagreb, Croatia

[*]*Corresponding author: jjacobs2@ucsc.edu*

Under review in Marine Ecology Progress Series

D29. Additional result: Scientific paper under review

https://doi.org/10.5194/egusphere-2025-6256

29 Dec 2025

Modelling primary production: multitude of theories, or multitude of languages?

Jozef Skákala, Shubha Sathyendranath, Yuri Artioli, Deep S. Banerjee, Heather Bouman, Robert J. W. Brewin, Momme Butenschön, Stefano Ciavatta, Stephanie Dutkiewicz, Yanna Fidai, David Ford, Grinson George, Karen Guihou, Bror Jönsson, Marija Bačeković Koloper, Žarko Kovač, Lekshmi Krishnakumary, Gemma Kulk, Charlotte Laufkötter, Gennadi Lessin, Jann Paul Mattern, Angélique Melet, Alexandre Mignot, David Moffat, Fanny Monteiro, Mayra Rodriguez Bennadji, Cécile Rousseaux, Ranjini Swaminathan, Osvaldo Ulloa, and Jerry Tjiputra

Under review in Ocean Science

D30. A new method for parameter estimation implemented

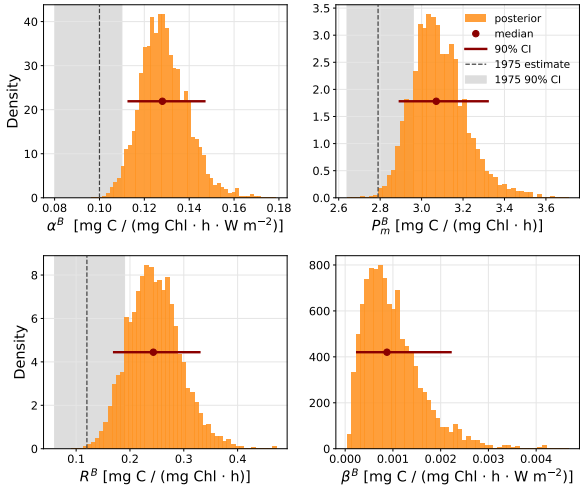

D31. New digitized historical data collected

In collaboration with **Dr. Andrew Erwin and Dr. Mohammad Amirian** from **Dalhousie University in Canada**, access to digitized historical data of experimental measurements of the dependence of photosynthesis on light has been achieved. We now have access to a digitized **dataset totaling 107,256 individual incubations**.

Primary production measurements in the Adriatic during 2025

In situ primary production measurements were conducted at the following stations:

Kašetla bay:
20.1., 28.2., 28.3., 11.4., 14.5., 23.7., 28.8., 4. 10., 29. 10., 20. 11., 11. 12.

Stončica station:
21.1., 24.2., 29.3., 12.4., 24.7., 31.8., 19.11., 10. 12.

Papers published in 2025

JGR Oceans

RESEARCH ARTICLE

10.1029/2024JC021415

Key Points:

- Interaction of phytoplankton with the underwater light field sets up a bio-optical feedback mechanism creating constants of motion
- A new differential equation shows that the light intensities at both the compensation depth and the critical depth are constants of motion
- Mixed-layer depth acts as the bifurcation parameter, and the critical depth is identified as the bifurcation point

Correspondence to:

Ž. Kovač,

zkovac@pmfst.hr

Citation:

Kovač, Ž., & Sathyendranath, S. (2025). Critical times for the critical depth theory. *Journal of Geophysical Research: Oceans*, *130*, e2024JC021415. https://doi.org/10.1029/2024JC021415

Critical Times for the Critical Depth Theory

Žarko Kovač[1] and Shubha Sathyendranath[2]

[1]Faculty of Science, University of Split, Split, Croatia, [2]National Centre for Earth Observations, Plymouth Marine Laboratory, Plymouth, UK

Abstract Critical Depth Hypothesis is arguably one of the longest standing biophysical theories in oceanography and is the earliest mathematically formulated theory aimed at explaining the phenomenon of phytoplankton blooms. It introduces a depth horizon, termed the critical depth, at which the integrated primary production from the surface to that depth equals the integrated loss terms within the same layer. In mixed layers deeper than the critical depth, losses dominate photosynthesis and vice versa. A related horizon in case of week mixing is the compensation depth, where the rate of photosynthesis matches the loss rate. In this paper, the effect of phytoplankton light attenuation on the critical depth is examined, showing that it creates a bio-optical feedback in the model. A new differential equation, derived for the time evolution of the compensation depth reveals that the light intensities at both the compensation depth and the critical depth are constants of motion. Exact solutions for average and total mixed layer biomass at steady state are derived, and their stability properties are analyzed. An existence of a bio-optical bifurcation is shown, in which the mixed layer depth acts as the bifurcation parameter and the critical depth is identified as the bifurcation point. Transients between steady states are also explored, and it is shown that the relation between the initial condition and the final steady state is paramount in determining whether a shallowing or deepening of the mixed layer will lead to a rise or a decline in biomass over time.

Published in Journal of Geophysical Research: Oceans

Papers published in 2025

Biogeosciences, 22, 3253–3278, 2025
https://doi.org/10.5194/bg-22-3253-2025

Biogeosciences Open Access EGU

Simulating vertical phytoplankton dynamics in a stratified ocean using a two-layered ecosystem model

Qi Zheng[1], Johannes J. Viljoen[1], Xuerong Sun[1], Žarko Kovač[2], Shubha Sathyendranath[3], and Robert J. W. Brewin[1]

[1]Centre for Geography and Environmental Science, Department of Earth and Environmental Sciences, Faculty of Environment, Science and Economy, University of Exeter, Cornwall, UK
[2]Faculty of Science, University of Split, Rudera Boškovića 33, 21000 Split, Croatia
[3]National Centre for Earth Observation, Plymouth Marine Laboratory, Plymouth, UK

Correspondence: Qi Zheng (q.zheng2@exeter.ac.uk)

Received: 8 November 2024 – Discussion started: 29 November 2024
Revised: 18 March 2025 – Accepted: 9 April 2025 – Published: 10 July 2025

Abstract. Phytoplankton account for around half of planetary primary production and are instrumental in regulating ocean biogeochemical cycles. Around 70 % of the oceans is characterized by either seasonal or permanent stratification. In such regions, it has been postulated that two distinct planktonic ecosystems exist, one that occupies the nutrient-limited surface mixed layer and another that resides below the mixed layer in a low-light, nutrient-rich environment. using two vertically separated planktonic ecosystems. Nevertheless, simulating the ecosystem in the subsurface layer was more challenging than the ecosystem in the surface mixed layer as less is known about model parameters and processes due to a lack of measurements, suggesting that more work is needed to study controls on subsurface planktonic communities.

Published in Biogeosciences

PHOTOCLIM

PHOTOCLIM.ORG

HrZZ

Croatian Science Foundation

Thank you!